Advanced Steel Construction – Vol. 21 No. 2 (2025) 147–156
DOI:10.18057/IJASC.2025.21.2.6

STUDY ON SELF-VIBRATION CHARACTERISTICS AND SEISMIC RESPONSE OF LARGE-OPENING DRUM-HONEYCOMB-TYPE QUAD-STRUT SUSPEND- DOME STRUCTURE

Hong-Wei Tu [1], Hui Lv [1, 2, *], Shi-Lin Dong [2, 3], Zhong-Yi Zhu [4] and Lian Shao [1]

[1] *College of Civil Engineering and Architecture, Nanchang Hangkong University, Nanchang 330063, China*
[2] *Space Structures Research Center, Zhejiang University, Hangzhou 310058, China*
[3] *Zhejiang Provincial Key Laboratory of Space Structures, Zhejiang University,Hangzhou 310058, China*
[4] *Beijing Institute of Architectural Design, Beijing 100045, China*
** (Corresponding author: E-mail: lvhui@nchu.edu.com)*

ABSTRACT

The large-opening drum-honeycomb-type quad-strut suspend-dome structure is a new type of suspend-dome structure, which was improved from the traditional cable dome structure. It replaces the top chord of the cable dome with seamless steel pipes. The structure combines the characteristics of the suspend-dome and the cable dome. The bottom chord nodes connects four struts, two inclined cables and one ring cable. The Ansys finite element model is established to analyze the influence of initial prestress, rise-span ratio, thickness-span ratio, opening span and bottom chord arrangement schemes on the natural vibration characteristics of the structure, and three seismic waves are selected to analyze the seismic response of the structure. The results show that the 1-50 order natural frequency range of the structure is 1.038-19.796, the stiffness of the outer ring is stronger than that of the inner ring, the horizontal stiffness is stronger than the vertical stiffness, and the overall stiffness of the structure is good. The initial prestress, thickness-span ratio and opening span have great influence on the self-vibration frequency, while the rise-span ratio and the bottom chord arrangement schemes have the least influence. The seismic response analysis shows that the peak values of vertical nodes displacement are -44.75mm, -47.40mm and -45.27 mm, respectively, which are far less than the allowable deflection limit, the peak internal force coefficients of the members are 1.82%, 6.53% and 7.49%, respectively, and the variation range is within the allowable range, The large-opening drum-honeycomb-type quad-strut suspend-dome structure has good structural stiffness, and the strength of the inner ring members should be appropriately strengthened to resist the dynamic effects such as earthquake.

ARTICLE HISTORY

Received: 7 August 2024
Revised: 24 December 2024
Accepted: 1 January 2025

KEYWORDS

Building structure;
Large-opening drum-honeycomb-type quad-strut suspend-dome;
Finite element analysis;
Self-vibration characteristics;
Seismic response

1. Introduction

As an important branch in the field of construction, large-span space structures benefit from the extensive use of prestressing technology. Suspend-dome structure is an important member of long-span string structure system, which is mainly composed of rigid top-chord reticulated shell, flexible bottom-chord high-strength cable and intermediate brace connection, which combines the structural characteristics of a single-layer mesh shell and a cable dome, and possesses the advantages of low cost, beautiful modeling, high structural rigidity, and low construction difficulty[1]. At the end of the last century, the Japanese scholar Kawaguchi put forward the new space structure system of Suspend-dome[2], which was introduced into China at the beginning of this century, and has been widely used in various types of large-scale public venues in China. For example, the badminton gymnasium for 2008 Olympic Games[3], Guiyang Olympic sport center[4], Zhangjiajie Circus City main stadium with suspended substructure suspend-dome structure[5]. In recent years, with the continuous development and advancement of suspend-dome, more and more complex structural forms have been put forward and applied in practical projects, such as Tianjin University of Traditional Chinese Medicine stadium project[6], conjoined suspend dome structure of Zhaoqing New District stadium[7], and loop-free suspend-dome after removal cables [8].

The difference between the traditional cable dome structure and the suspend-dome structure is that it is a flexible structure, and when the structure is subjected to large loads, the top chord spine cable is prone to slacken and quit working, resulting in a decline in the stiffness of the structure, excessive displacement and other phenomena. And because of its use of flexible cable material, it is difficult to control the accuracy of tensioning construction, and the construction is more difficult. Scholars at home and abroad have been carrying out research on the perfection and improvement of this kind of structure.

In 2005, academician Dong Shilin's team[9]proposed Kiewitt cable dome and hybrid new dome based on the advantages and disadvantages of the existing cable dome forms, and comprehensively considered the structural topology and mechanical characteristics. The prestress level was theoretically calculated using the overall feasible prestress theory. This example can provide theoretical support for the improvement of the cable dome structure. In 2010 , Dong Shilin's team[10] proposed a spatial structural form combining the top chord single-layer mesh shell and the bottom flexible cable structure, which developed the stress characteristics of the cable dome structure and reduced the difficulty of laying panels at the later stage of construction, and applied the method to sunflower-type, rib-ring-type, and Kiewitt-type cable domes. In 2017, Zhang Ailin[11] improved the traditional ridge-rod ring-braced cable dome structure, replaced all the flexible cables of the top reticulated shell with rigid rods, and proposed a new type of ridge-rod ring-braced cable dome. The static and parameter analysis was carried out, which solved the shortcomings of the traditional cable dome structure, such as the relaxation of the top chord cable under compression and the large number of inclined cables, and enriched the selection of the cable dome structure.In 2019, Sun Guojun[12] proposed a rigid support dome on the basis of the cable dome, replacing all the cables in the bottom part of the original cable dome with rigid tie rods, which solved the problem of difficult construction positioning of the prototype structure. The self-vibration characteristics test was carried out to study the feasibility of the dome.

The above scholars' research on the cable dome and suspend-dome structure has made up for the lack of such space structures in China, and enriched the selection and program of space structures. Based on the above scholars' attempts and researches on this kind of space structure, this paper proposes a large-opening drum-honeycomb-type quad-strut suspend-dome structure, which was based on the improvement of the traditional cable dome with the same topological configuration[13], which possesses stronger structural stiffness and deformation resistance, and is able to solve the some of the intrinsic deficiencies of the cable dome structure, according to which, large-opening drum-honeycomb-type quad-strut suspend-dome structure is established, and an Ansys finite element model is developed to study the structure under load. Accordingly, the Ansys finite element model is established, and the self-vibration characteristics under the load state and the influence of its structural parameters on the self-vibration frequency of the structure are studied, as well as the seismic response, to explore the feasibility of the large-opening drum-honeycomb-type quad-strut suspend-dome structure, and to help improve the theoretical basis of the new structural system.

2. large-opening drum-honeycomb-type quad-strut suspend-dome structure

2.1. Finite element modeling

The plan and section of the large-opening drum-honeycomb-type quad-strut suspend-dome structure are shown in Fig.1 and Fig2. The overall structure

consists of top chord mesh shell and bottom chord, with the top chord mesh shell mainly divided into ridge rods (JG) and ring rods (HG), and the bottom chord mainly divided into struts (CG), ring cable (HS), and inclined cables (XS). As can be seen from Fig.1, the bottom chord nodes are located below the hexagonal honeycomb grid, and each bottom chord node connects a total of four struts and two inclined cables, and passes through one ring cable.

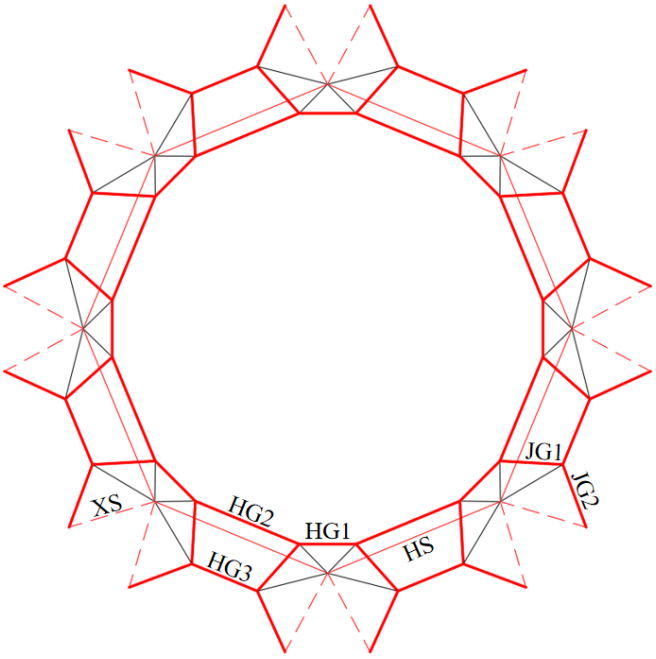

Fig. 1 Planar gragh

The arrangement of the bottom chord nodes is shown in Fig.2, where *L* is the span, *h* is the thickness of the mesh shell, *f* is the sagittal height of the mesh shell, 1a, 1b and 2a are the top chord nodes of the structure, and 1' is the bottom chord node.

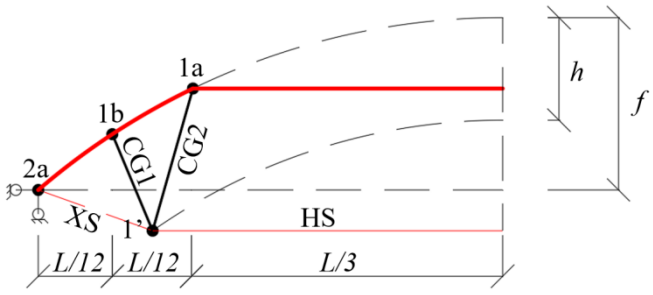

Fig. 2 Sectional graph

2.2. Finite element modeling

Ansys finite element software is applied to analyze the self-vibration characteristics and dynamic time history analysis of the large-opening drum-honeycomb-type quad-strut suspend-dome structure, and to investigate the mechanical response analysis of the model under the loading condition. The span of the large-opening drum-honeycomb-type quad-strut suspend-dome structure is set to be 120m, the ring equivalent fraction is 16, the rise-span ratio and the thick-span ratio are taken as 0.10, the sagittal height is 12m, and the opening diameter is 80m. The ridge rod, ring rods and struts are all made of Q235B seamless steel pipes, with yield strength of 234 Mpa and modulus of elasticity of 2.06×105 Mpa, and the inclined cable and ring cable are made of high-strength stranded wires, with tensile strength of 1,270 Mpa and modulus of elasticity of 1.90×105 Mpa.The cross-section dimensions of the selected members and the length-to-slender ratio are in line with the specification requirements.

The peripheral support of the structure adopts the fixed hinge support, and Link180 unit is applied to simulate the top chord and bottom chord respectively, and the Keyopt function of Ansys finite element software is used to set up the tensile and compressive members, only tensile members and only compressive members. In the subsequent analysis of self-vibration characteristics, it is necessary to apply load to the structure, in which the constant load is 0.5kN/m^2 and the live load is 0.6kN/m^2. Specify the analysis type as dynamic analysis, and turn on the large deformation effect and stress stiffening. The bottom chord cable system is an active tension system, while the top chord mesh shell is a passive tension system, so only the initial prestress of the bottom chord cable system needs to be determined, and then the prestress distribution of the top chord mesh shell can be obtained. The initial prestress distribution of the bottom chord cables can be calculated according to the calculation method used in the literature of [14]，[15]and[16], In this paper, the concept of overall feasible prestress is used to calculate the initial prestress value of various components. For the suspend-dome structure, it is necessary to find the general prestress state X, find a set of *a*, so that the prestress of the same set of components is equal, and the prestress modal combination can correctly obtain the initial prestress. Let *X* be the overall feasible prestress mode. according to the balance equations of each node, the initial prestress values of various components are obtained,

$$T_1 + T_2\alpha_2 + \ldots + T_s\alpha_s = X \tag{1}$$

In Eq. (1), *a* is 1 and *X* is the unit feasible prestress. For the structure with n component types, it can be written as :

$$X = \{x_1 x_2 x_3 \ldots x_i x_i x_i \ldots x_n x_n x_n\}^{\mathrm{T}} \tag{2}$$

Let x_i be the *i*-class component, then (2) can be organized as follows :

$$T_1\alpha_1 + T_2\alpha_2 + \ldots + T_s\alpha_s - X = 0 \tag{3}$$

Briefly :

$$\tilde{T}\,\tilde{\alpha} = 0 \tag{4}$$

Of which :

$$\tilde{T} = [T_1 T_2 \ldots T_i \ldots T_s - e_1 - e_2 \ldots - e_n] \tag{5}$$

In Eq. (5), T_i is the independent self-stress mode, the base vector e_i is the *i*-type member, the struts axial force is -1 (the cable axial force is +1), and the axial force of the remaining members is 0. The unknown number $\tilde{\alpha}$ is :

$$\tilde{\alpha} = \{\alpha_1\alpha_2 \ldots \alpha_s x_1 x_2 \ldots x_n\}^{\mathrm{T}} \tag{6}$$

The singular value decomposition of $\tilde{T}$ can be obtained :

$$\tilde{T} = USV^{\mathrm{T}} \tag{7}$$

In Eq. (7), *U* and *V* are the left and right singular vector matrices of $\tilde{T}$, respectively, and *S* is the singular value matrix. Suppose the rank of *T* is r, then the r+1 column to s+n column vector in the right singular vector matrix *V* is the solution of $\tilde{\alpha}$, and the initial prestress corresponding to each group of components is the value of r+1 column to s+n column in $\tilde{\alpha}$. So far, the overall feasible prestress of the structure can be obtained. The initial prestress value of the large-opening honeycomb quad-strut suspend-dome structure is shown in Table 1.

Table 1
Component Names and Specifications

Name of members	Section size (m^2)	Prestress (kN)
JG1	0.0217	4394
JG2	0.0274	5547
CG1	0.0184	-1266
CG2	0.0159	-845
HG1	0.0487	9854
HG2	0.0372	7134
HG3	0.0235	4752
XS	0.0123	4351
HS	0.0282	10000

The numerical analysis model is generated, as shown in Fig.3.

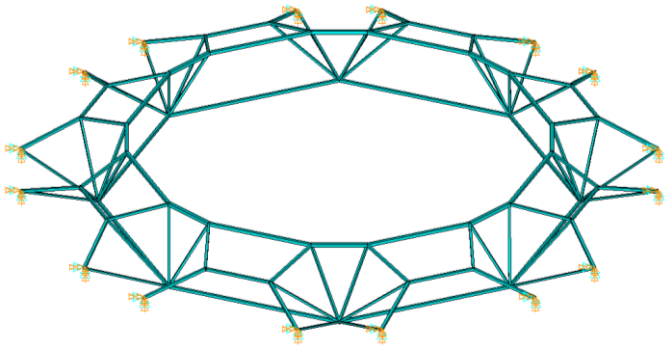

Fig. 3 Ansys Model

3. Structural self-vibration characterization

3.1. Self-vibration properties

Taking the structural parameters described in the previous section as an example, 1 times constant load and 0.5 times live load are applied to the structure, and the self-vibration frequency and vibration pattern diagrams of the large-opening drum-honeycomb-type quad-strut suspend-dome structure are observed through the self-vibration modal analysis of the structure in the first 50th order, which is shown in Fig.4. The self-vibration frequency of the structure in the 1st-50th order ranges from 1.04 to 19.79, and the self-vibration frequency is high, and the self-vibration frequency in the 1st-16th, 23rd-29th, and 44th-48th orders rises slowly, and the self-vibration frequency in the three stages rises in a stepwise manner, and the low-order self-vibration frequency rises slowly and is distributed relatively densely, while the self-vibration frequency of the high-order rises larger and is distributed more sparsely. From the topological configuration of the structure, the structure is centrosymmetric, so the self-vibration frequencies basically appear in pairs.

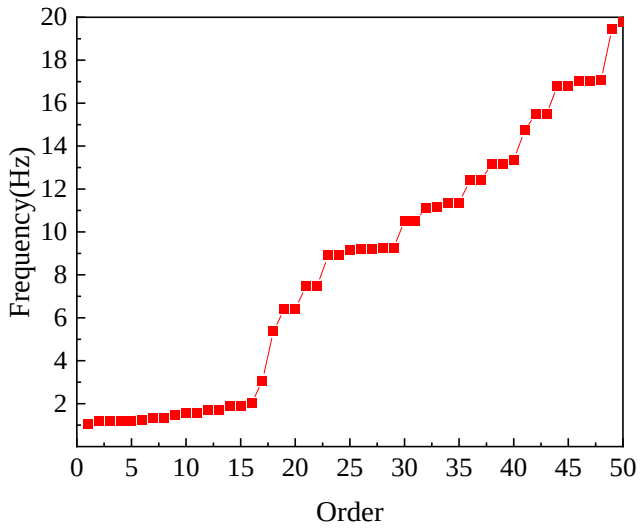

Fig. 4 Structural self-vibration frequency

Mass participation coefficient is also an important parameter in structural dynamics analysis, which is mainly used to measure the degree of mass participation in natural vibration in each direction of each mode. As shown in Fig 5, the mass participation coefficient of the structure in the ROTZ direction is the largest in the 0-6 order vibration. After the 6th order, the mass participation coefficients in the ROTX and ROTY directions are also greatly improved. After the 16th order, the mass participation coefficients in the Z, X and Y directions have been greatly improved. When the 50th order is reached, the cumulative mass participation coefficients in all directions reach 1. It can be seen that the ROTX, ROTY and ROTZ directions are the most involved in the natural vibration, followed by the Z direction.

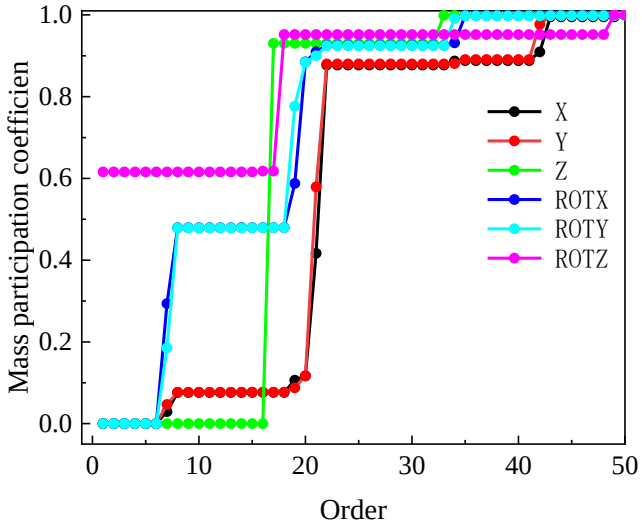

Fig. 5 Mass participation coefficien

In the structural vibration pattern in Fig.6, the 1st order vibration pattern is mainly for the horizontal torsion of the inner and outer ring rod, and the vertical displacement is small; the 2nd and 3rd order vibration pattern is for the structural symmetry of the 4 places of the ring rod vertical staggered vibration, and the structural torsion did not occur; the 4th and 5th order vibration pattern is for the structural symmetry of the vertical staggered vibration of the two places, and the structural torsion did not occur; the 6th order vibration pattern is for the inner circle of the ring rod of every grid staggered vibration is mainly up and down; The 7th and 8th order vibration patterns are symmetrical two-point vertical torsion. The 9th order vibration mode is dominated by the adjacent 1b node staggered vertical vibration; the 10th order vibration mode is the structure symmetrical four-point 1b node vertical vibration. It can be concluded that the deformation points of the low-order vibration mode are mainly distributed near the inner ring bar, and the deformation points are gradually transferred to the outer ring as the order rises. As far as the large-opening drum-honeycomb-type quad-strut suspend-dome structure is concerned, the stiffness of the inner ring is lower than that of the outer ring, the vertical stiffness is weaker than that of the horizontal stiffness, and the overall stiffness of the structure is better.

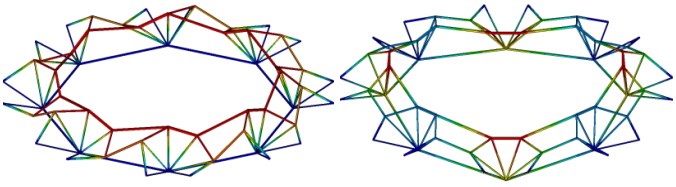

（a）1st（1.0376）　（b）2 and 3th（1.1728）

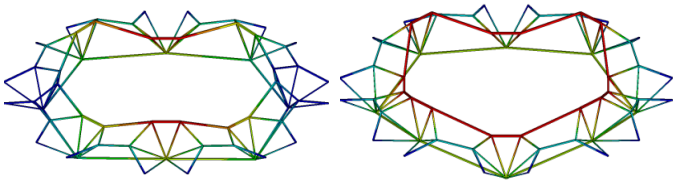

（b）4 and 5th（1.2073）　（d）6th（1.2304）

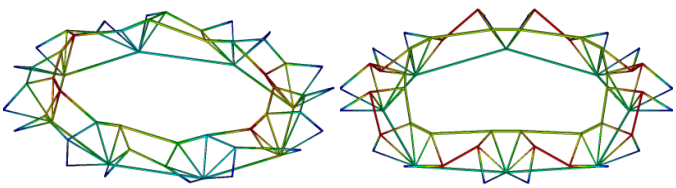

（e）7 and 8th（1.3546）　（f）9th（1.4804）

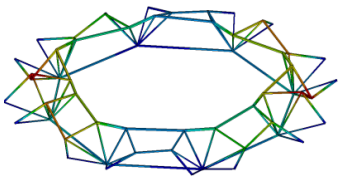

（g）10th（1.5451）

Fig. 6 Structural vibration pattern

3.2. parametric analysis

The large-opening drum-honeycomb-type quad-strut suspend-dome structure has a variety of structural parameters such as initial prestress, rise-span ratio, thickness-span ratio, opening diameter, and bottom chord arrangement. For this kind of large-span spatial steel structure, its structural parameters have a certain degree of influence on the structural performance. Therefore, in order to further investigate the structural performance of the large-opening drum-honeycomb-type quad-strut suspend-dome structure, it is necessary to conduct parametric analyses of the structure to investigate the degree of influence of each type of parameter on the structural self-vibration characteristics. The following parametric analyses were performed under the loading conditions in the previous section.

3.2.1. Initial prestress

The initial prestress of the large-opening drum-honeycomb-type quad-strut suspend-dome structure is set to be 1P, and the structural self-vibration frequency of the structure is investigated at prestress levels of 0.5-3.0P in steps of 0.5P. With other parameters kept constant, it can be concluded from Fig.7 that under the six initial prestress conditions, all six curves show the same upward trend, and the curves have no obvious difference in the frequency in the 1-17th order, and the frequency is kept at a lower level with a slower upward trend; in the 18th-19th order the curves have an obvious upward trend, and they start to show an obvious dispersion in the 18th order up to the 50th order, and then in the 20th- 50th order, the curves basically show the same rate of increase, and at the same order, the self-vibration frequency of 0.5-3.0P increases sequentially. Under the same conditions, the structural stiffness rises with the increase of prestress level.

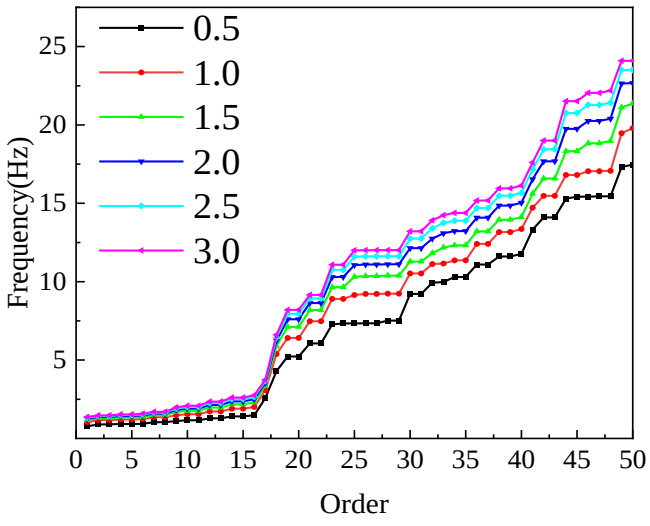

Fig. 7 Prestress level

3.2.2. Rise-span ratio

The rise-span ratio is the ratio of structural sagittal height to span, which is an important parameter of space structure. According to the structural characteristics of the large-opening drum-honeycomb-type quad-strut suspend-dome structure, the rise-span ratio can be categorized into 0.4-0.16, which can be derived from Fig.8, where the distribution of the curves is more intensive and the overall difference is smaller. In order 1-17, the curves have basically the same upward trend and the trend is slower; in the interval of order 18-21, the curves basically overlap and the upward trend is faster; in the interval of order 22-30 the curves are obviously dispersed, and the rise-span ratio is the lowest in order 0.16-0.14, the highest in order 0.06-0.08, and the rest are in the middle; in the interval of order 31-40 the curves enter into overlap, and then they are gradually dispersed after order 41 . It is concluded that the effect of structural rise-span ratio on structural self-vibration characteristics is insignificant.

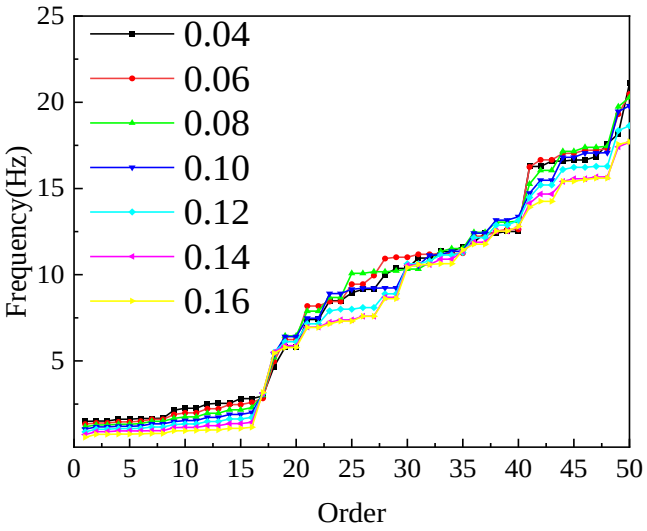

Fig. 8 Rise-span ratio

3.2.3. Thickness-to-span ratio

The thickness-to-span ratio is the ratio of the thickness of the structure to the span, and in the large-opening drum-honeycomb-type quad-strut suspend-dome structure, the thickness-to-span ratio will be between 0.06-0.16. From Fig.9, it can be concluded that there is no much difference between the curves in the 1-17 order interval; the curves are scattered obviously after that, and their frequencies gradually increase with the thickness-to-span ratio of 0.06-0.12, and only individual dispersion occurs with the thickness-to-span ratio of 0.14-0.16, with the frequency of the size of the structure being basically the same. From this, the influence of the structure's thickness-to-span ratio on the self-vibration characteristics is the most obvious.

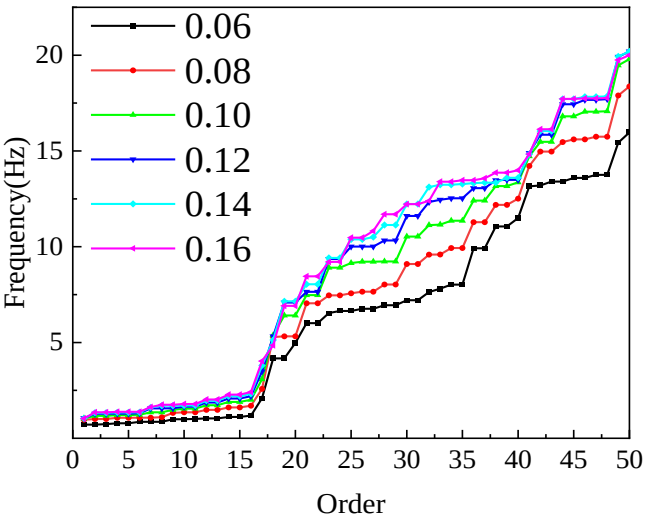

Fig. 9 Thickness-span ratio

3.2.4. Opening diameter

Since this type of suspend-dome structure has a large opening, the span of the opening is also an important morphology parameter, and within the allowable range of the opening size of this type of suspend-dome structure, the diameter of the opening of 60-100m is taken as a parameter to be analyzed. From Fig.10, it can be concluded that the curves show the trend of dispersion from the beginning, and in the interval of order 1-17, the curves rise slowly, and then rise faster, and the curves do not overlap significantly during the whole period, and from the overall pattern, the self-vibration frequency basically increases with the expansion of the structural diameter of the openings.

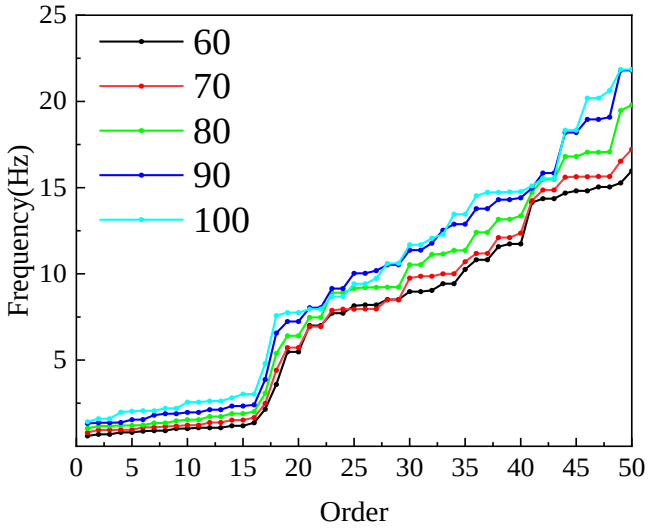

Fig. 10 Opening diameter

3.2.5. Bottom chord arrangement schemes

The large-opening honeycomb quad-strut suspend-dome structure has three bottom chord arrangement schemes, that is, the distance between the bottom chord node and the center of the structure. The distance gradually increases with the scheme 1-3, and the angle between the struts (CG) and the horizontal plane also decreases. From Fig.11, it can be concluded that the curves of the three bottom chord arrangement schemes do not show obvious dispersion and are basically in the same trend, with individual small dispersion only in the middle section and the rear end, but it can still be seen that there are minor differences in the bottom chord arrangement schemes. It is concluded that its bottom chord arrangement schemes has the least influence on the self-vibration characteristics of the structure.

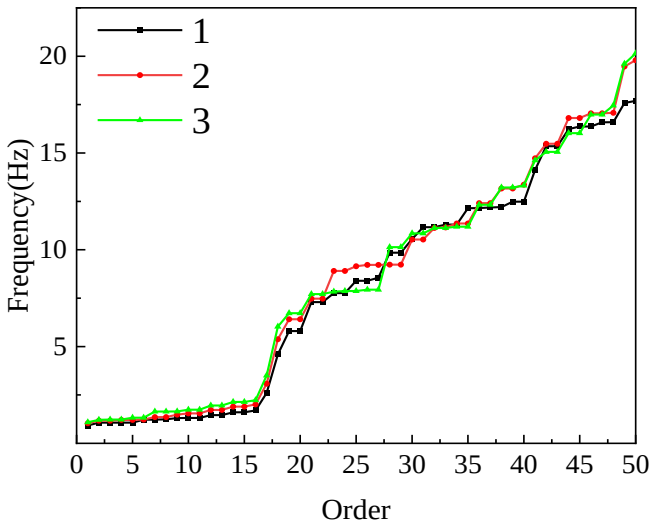

Fig. 11 Bottom chord arrangement schemes

Taken together, the magnitude of the influence of each parameter on the self-vibration frequency of the structure can be classified as thickness-to-span ratio > prestress level > opening diameter > rise-span ratio > bottom chord arrangement schemes.

4. Structural seismic response analysis

The large-opening drum-honeycomb-type quad-strut suspend-dome structure is a tension system consisting of an top single-layer mesh shell and bottom ring cables. As a new type of suspend-dome structure improved from the traditional cable dome structure, and therefore it is necessary to perform seismic response analysis. In this section, the structure with parameters of prestress level 1P, rise-span ratio 0.10, thickness-span ratio 0.10, opening diameter 80m and bottom chord arrangement scheme 2 is analyzed.

4.1. Seismic wave selection

In this section, the seismic time-course analysis is carried out for the large-opening drum-honeycomb-type quad-strut suspend-dome structure, and according to the GB50011-2010 "Code for Seismic Design of Buildings" 5.1.2[17], the structure should be selected with at least two actual recorded seismic waves and one artificially generated by the simulation when the seismic response analysis is carried out.

The seismic effects is related to the spatial location and the structure itself, the seismic conditions in this paper in accordance with the Areas with seismic fortification intensity of level 8 for calculation, the maximum ground acceleration of 70cm/s^2. and according to the provisions of JGJ7-2010 "Technical Specification for Space Frame Structures" 4.4.10[18], the value of the damping ratio is selected as 0.02, as well as the first and second order of the self-vibration frequency for the calculation of the Rayleigh damping coefficient. In this paper, the classical EI-Centro seismic wave, Tianjin Ninghe seismic wave and an artificial seismic wave are selected for seismic response simulation, and the original seismic wave is shown in Fig.12 to Fig.14, in which the peak acceleration of the EI-Centro seismic wave is 341.7 cm/s^2, the peak acceleration of the Tianjin Ninghe seismic wave is 145.8 cm/s^2, and the peak acceleration of the artificial seismic wave is 817 cm/s^2. The duration of all three seismic wave inputs is 20s.

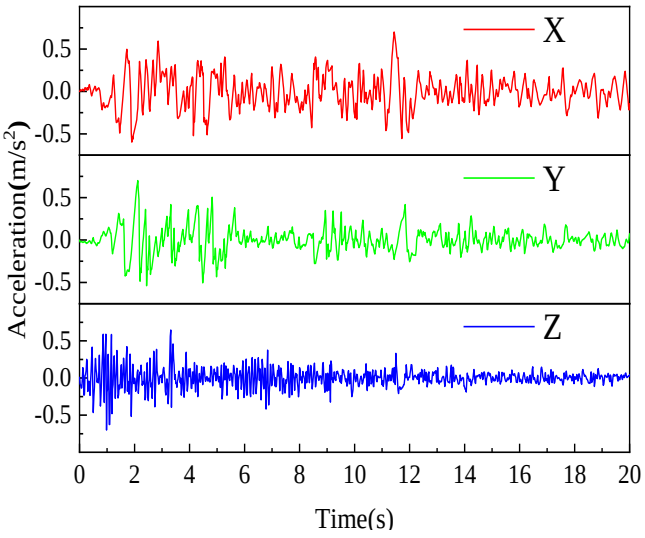

Fig. 12 EI-Centro seismic wave

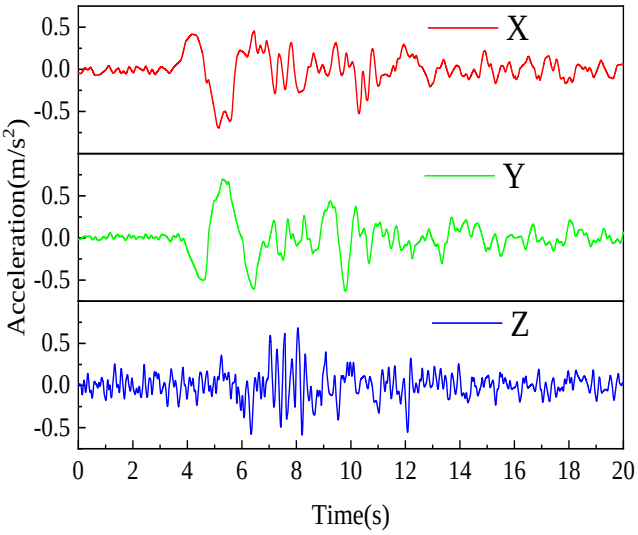

Fig. 13 Tianjin Ninghe seismic wave

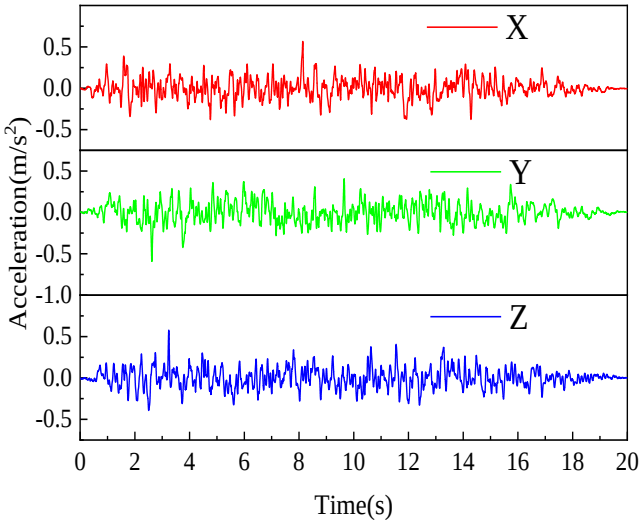

Fig. 14 Artificial seismic wave

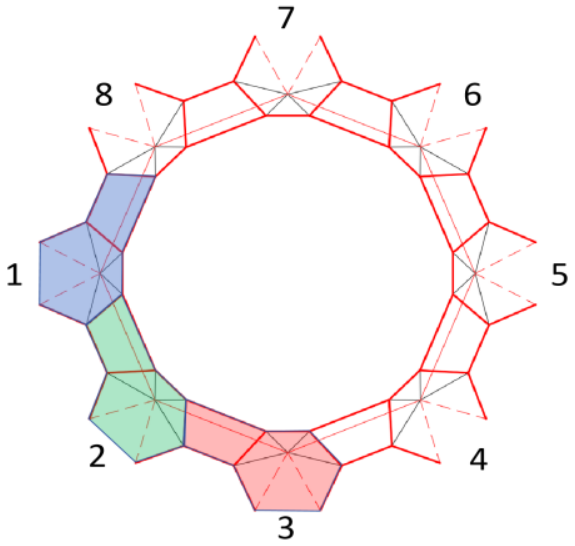

Fig. 15 Sub-structures

When conducting seismic time-course analysis on structures, The original seismic wave cannot be directly used for calculation, the amplitude should be adjusted according to equation (1). And the three seismic waves are three-way seismic waves, the peak acceleration before input should be adjusted according to the requirements of the specification, the X direction, the Y direction and the Z direction in accordance with the ratio of 1:0.85:0.65.

$$A'(t) = (A'_{max}/A_{max})A(t) \tag{8}$$

In Eq.(8). $A'(t)$ *is* the seismic time-course curve. A'_{max} is the peak acceleration of the curve. which is the peak acceleration of a magnitude 8 multiple-occurrence earthquake selected in the code. A(t) is the original seismic time-course curve. A_{max} is the peak acceleration of the original time-curve of the earthquake.

The large-opening drum-honeycomb-type quad-strut suspend-dome structure is divided into 8 sub-structures, and its sub-structures are schematically shown in Fig.15. For space limitation reasons, specific sub-structures will be selected for analysis in the seismic response analysis in this chapter.

4.2. Structural displacement response

For space limitation reasons, in this section, the analysis is based on EI-Centro seismic wave response and nodes 1a, 1b and 1' of the first, second and third sub-structure are selected for displacement analysis. From Fig.16, it can be concluded that among the three nodes in each sub-structure, the displacement in the Z direction is the largest, followed by the X direction and the Y direction is the smallest, indicating that the seismic action has less effect on the structure in the X and Y directions, and due to the effect of the structure's self-weight, the initial displacement in the Z direction of the three nodes is larger, and the curve patterns in the three directions are basically similar to those of the EI-Centro seismic acceleration curves.

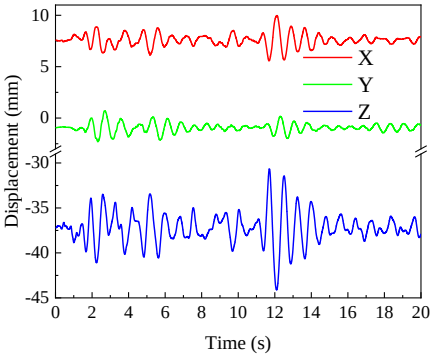

（a）The 1a of first sub-structure

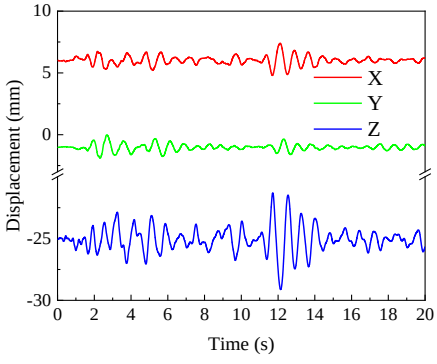

（b）The 1b of first sub-structure

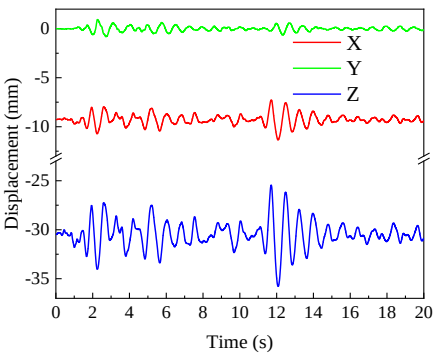

（c）The 1’ of first sub-structure

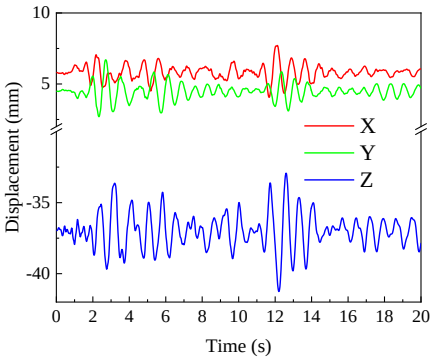

（d）The 1a of second sub-structure

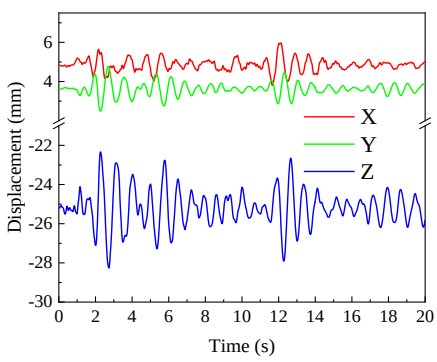

（e）The 1b of second sub-structure

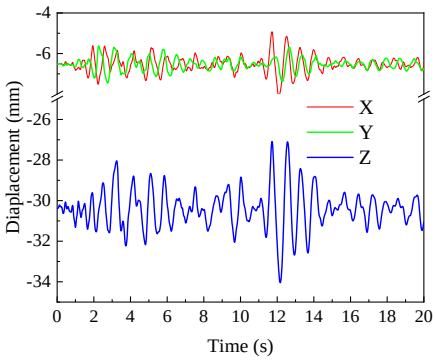

（f）The 1’ of second sub-structure

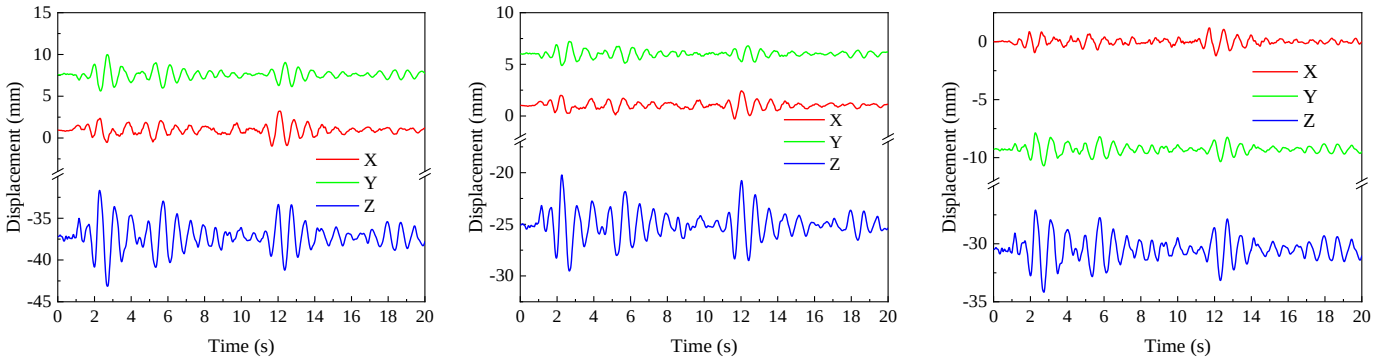

（g）The 1a of third sub-structure （h）The 1b of third sub-structure （i）The 1’ of third sub-structure

Fig. 16 Nodal displacement time-course curves under EI-Centro seismic waves

Table 2
Vertical displacement of nodes

Seismic waves	Nodes	Maximum displacement (mm)	Time (s)
EI-Centro seismic wave	1a	-44.75	12.06
	1b	-30.58	12.06
	1’	-35.79	12.08
Tianjin Ninghe seismic wave	1a	-47.40	0.44
	1b	-32.82	0.44
	1’	-38.09	0.44
Artificial seismic wave	1a	-45.27	20.00
	1b	-31.26	20.00
	1’	-36.52	20.00

The peak displacement of the nodes in the X and Z directions of the first substructure appears at about 12s, and the peak displacement of the nodes in the Y direction appears at about 2.5s. The initial displacement in the X direction has a certain offset, and the absolute value is between 5-10 mm. The initial displacement in the Y direction is small, basically around 0. The peak time of node displacement in the X and Y directions of the second substructure is similar to that of the first substructure, and the initial displacement is offset, the offset of the two is similar, while the peak displacement of the 1b node in the Z direction is advanced to about 2.5s. The peak time of node displacement in X and Y directions of the third substructure is similar to that of the first substructure. The initial displacement offset of the X direction node is small, which is basically around 0. The initial displacement offset of the Y direction node is large, and the peak displacement of the three nodes in the Z direction is advanced to about 2.5 s. It can be concluded that under the action of earthquake, the substructures in the symmetry axis direction represented by 1-3 substructures produce uneven deformation, and the displacement response time of different substructures in the Z direction is also different. Under the action of horizontal seismic waves, the displacement in the X and Y directions is small, showing that the bottom chord quad-strut form of the large-opening honeycomb quad-strut suspend-dome structure has better lateral stiffness.

In Tab.2, under the action of each seismic wave, the peak Z direction nodal displacements are -44.75mm, -47.40mm and -45.27mm, which are much smaller than the permissible deflection limit of *Lc* / 300 specified in the GB50017-2017 "Standard for Design of Steel Structures" [19], which is 133.3 mm, and *Lc* is the total overhanging span.

4.3. Structural deformation response

The structural deformation reflects the stiffness change of the structure under seismic action. Fig.17 to Fig.19 shows the structural deformation of the structure under the action of each seismic wave, in Ansys the deformation is set as a displacement vector sum, which is the vector sum of X, Y and Z directions. As the structure under seismic action in the Z direction displacement is larger, the remaining two directions displacement is smaller, in Fig.19 can be seen, the three deformation diagrams to vertical displacement is dominated, and are biased to one side, the pattern is basically the same, the maximum deformation were 46.24mm, 48.95mm and 46.68mm. It shows that the structure has basically the same ability to resist vertical deformation under the action of three seismic waves, and shows good structural stiffness.

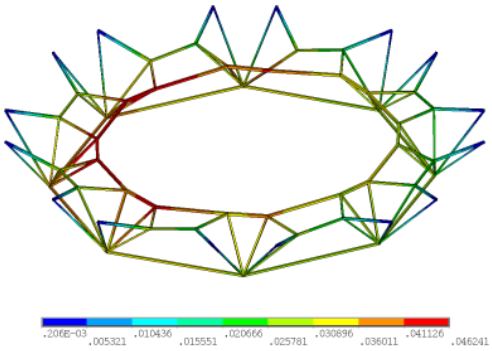

Fig. 17 EI-Centro seismic wave

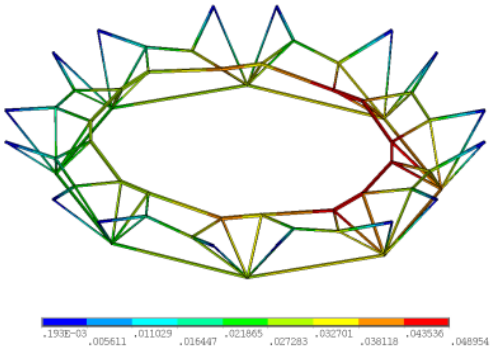

Fig. 18 Tianjin Ninghe seismic wave

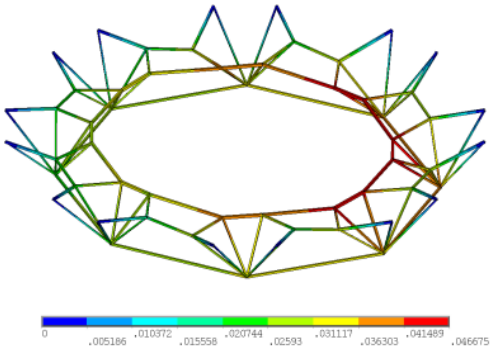

Fig. 19 Artificial seismic wave

4.4. Structural internal force response

In this section, the analysis is still based on the EI-Centro seismic wave response, and Fig.20 shows the various types of members in the first sub-structure, and Tab.3 shows the maximum internal force coefficients of the various types of rods and their rate of change under the three seismic waves. As shown in Fig.20, the time-course curves of the internal forces of the ridge rods and the ring rods are zigzag and dense, while those of the gusset rods, diagonal ropes, and ring cables are sparse, and the top chord mesh shell is a horizontal member, so it can be seen that the top chord mesh shell is more sensitive to seismic effects, while the struts, as a vertical member, have the second highest sensitivity to seismic effects, and the inclined cable and the ring cables, as a flexible material, are the least sensitive to seismic effects. Due to the effect of structural self-weight, the internal force of ridge rod and ring rod decreased compared to the initial prestress of the structure, while the struts, inclined cables and ring cables increased.

As shown in Tab.3, the peak coefficients of the internal forces of the members under the three seismic waves are 1.82%, 6.53%, and 7.49%, respectively, and their variations are within the allowable range. In the ridge rods, the peak internal force of JG1 is smaller than that of JG2; in the struts, the peak internal force of CG1 is smaller than that of CG2; in the ring rods, the peak internal forces of HG1 and HG2 are smaller than that of HG3; and the peak internal force of the ring cables is smaller than that of the inclined cables, so it can be seen that the closer the structure is to the inner circle of the members, the more obvious it is subjected to seismic effects. In the design of this type of structure, attention should be paid to the appropriate strengthening of the inner ring members to resist seismic effects.

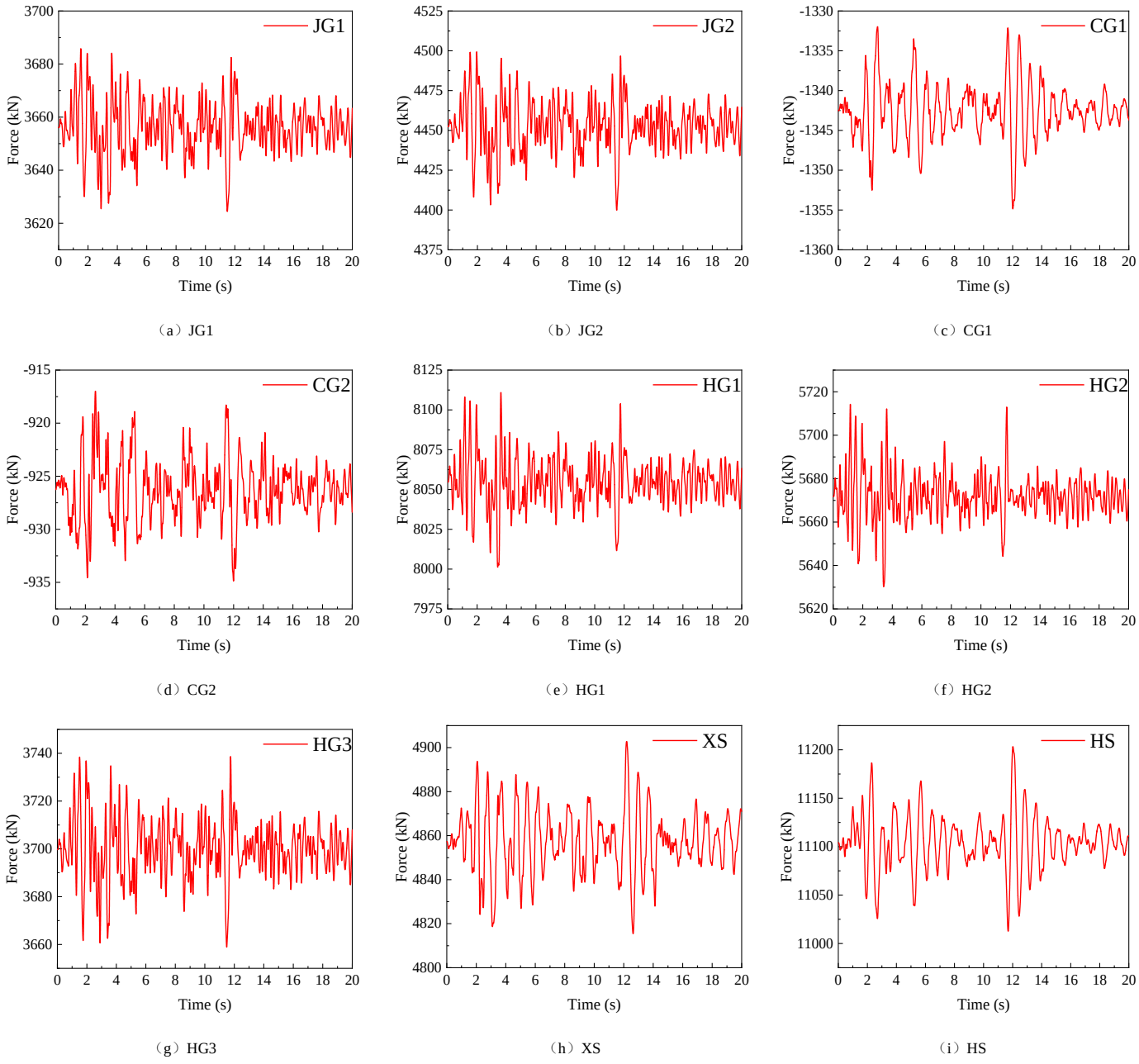

Fig. 20 Time-course curves of internal forces in members under EI-Centro seismic waves

Table 3
Internal force coefficients of members

Seismic waves	Members	Initial internal force coefficients	Maximum internal force coefficients	Rate of change
EI-Centro seismic wave	JG1	1.00	1.0085	0.85%
	JG2	1.00	1.0114	1.14%
	CG1	1.00	1.0100	1.00%
	CG2	1.00	1.0113	1.13%

	HG1	1.00	1.0072	0.72%
	HG2	1.00	1.0078	0.78%
	HG3	1.00	1.0112	1.12%
	XS	1.00	1.0182	1.82%
	HS	1.00	1.0090	0.90%
	JG1	1.00	1.0506	5.06%
	JG2	1.00	1.0647	6.47%
	CG1	1.00	1.0186	1.86%
	CG2	1.00	1.0653	6.53%
Tianjin Ninghe seismic wave	HG1	1.00	1.0324	3.24%
	HG2	1.00	1.0255	2.55%
	HG3	1.00	1.0595	5.95%
	XS	1.00	1.0249	2.49%
	HS	1.00	1.0126	1.26%
	JG1	1.00	1.0572	5.72%
	JG2	1.00	1.0732	7.32%
	CG1	1.00	1.0223	2.23%
	CG2	1.00	1.0749	7.49%
Artificial seismic wave	HG1	1.00	1.0360	3.60%
	HG2	1.00	1.0335	3.35%
	HG3	1.00	1.0671	6.71%
	XS	1.00	1.0298	2.98%
	HS	1.00	1.0098	0.98%

Note: The initial internal force coefficient for each member is 1.00, and the maximum internal force coefficient is equal to the ratio of the maximum internal force to the initial internal force

5. Conclusions

This paper applies the method of finite element analysis to investigate the self-vibration characteristics of the large-opening drum-honeycomb-type quad-strut suspend-dome structure proposed in this paper in the loading state with the effects of its structural parameters on the self-vibration frequency of the structure, as well as the seismic response, and the following conclusions are drawn through the comparative analyses:

(1) Under the condition of applying 1 times of constant load and 0.5 times of live load, the structure was subjected to the self-vibration modal analysis of the first 50 orders, and the self-vibration frequency of the structure in the range of 1.038-19.796 for the 1st-50th orders is higher, which indicates that its structural stiffness is better, and its self-vibration frequency occurs in pairs due to the centrosymmetric shape of the topological configuration of the structure. Its low-order frequency is more dense, and the rising trend is slower, and the overall self-vibration frequency shows a stepwise rise, while the middle and high-order frequency rises faster and is more sparsely distributed. In addition, the mass in the ROTX, ROTY and ROTZ directions is more involved in the whole process of natural vibration, followed by the Z direction.The first ten orders of the vibration pattern first appeared horizontal torsion, followed by vertical deformation, and vertical deformation points with the rise of the order gradually transferred to the outer ring. In terms of the large-opening drum-honeycomb-type quad-strut suspend-dome structure, the outer ring stiffness is stronger than the inner ring, and the horizontal stiffness is stronger than the vertical stiffness, and the overall stiffness of the structure is better.

(2) The influence of the large-opening drum-honeycomb-type quad-strut suspend-dome structure on the self-vibration frequency of the structure was investigated for different parameters such as initial prestress, rise-span ratio, thickness-span ratio, opening diameter, and bottom chord arrangement schemes. It is finally concluded that the initial prestress, thickness-to-span ratio, and opening diameter have a greater effect on the self-vibration frequency of the structure, while the rise-span ratio and bottom chord arrangement schemes have the least effect. The influence of each parameter on the self-vibration frequency of the structure can be categorized as thickness-to-span ratio > prestress level > opening diameter > rise-span ratio > bottom chord arrangement schemes.

(3) Finally, this paper selected EI-Centro seismic wave, Tianjin Ninghe seismic wave and an artificial seismic wave for seismic response simulation, and analyzed that the seismic action on the structure is the most obvious Z-direction displacement, the X and Y-direction displacement is smaller, and the other three initial displacements are shifted to different degrees. In addition, the maximum nodal displacements of the structure under seismic wave action are all much smaller than the allowable deflection limits of the code. The structure generally exhibits better lateral and vertical stiffness.

(4) From the deformation diagrams of the maximum displacement vector and the structure, the structure is mainly deformed in the vertical direction, and all of them are biased to one side, and the maximum deformation is small, which has better ability to resist the deformation of seismic action.

(5) From the time-course curves of internal force of each member of the structure, the mesh shell of the structure is more sensitive to seismic action, and the struts, inclined cables and ring cables are the least sensitive, and the peak internal force of each member has a smaller amount of change compared with the initial internal force. The closer the structure is to the inner ring, the larger the peak internal force coefficient is, and the more obvious the seismic effect is, so attention should be paid to strengthen the strength of the inner ring members to resist earthquakes and other effects.

(6) There are some deficiencies in the research of this paper. For example, it focuses on numerical simulation, but fails to carry out the model test of the suspend-dome structure to verify the accuracy and reliability of the numerical simulation. Therefore, it is necessary to further complete the experimental study of the structure when the conditions permit. As a large-span spatial structure, the cable-strut failure and progressive collapse of the structure need to be further explored.

References

[1] Zhao Wenyan, ZhaoChuang, Pan Wenzhi, et al. Research on the Temporary Support System for Super Large-Span Ribbed-Type Suspen-Dome [J]. Progress in Steel Building Structures, 2023, 25 (01): 98-104.

[2] Kawaguchi M, Abe M, Tatemichi I. Design, tests and realization of “suspend-dome” system[J]. Journal of the International Association for Shell and Spatial Structures, 1999, 40(3):179-192.

[3] Zhang Ailin, Ge Jiaqi, Liu Xuechun. Design and research of the large-span steel structure of the badminton gymnasium for 2008 Olympic Games [J]. Journal of Building Structures, 2007, (06)：1-9.

[4] Fu Shaohui, Zhang Ling. Architecture inlaid in the mountains-Guiyang Olympic Sports Center Planning and Main Stadium Design [J]. Architectural Journal, 2011, (09): 86-87.

[5] Shu ganping, Pan Rui, Wang Siqing, et al. Analysis and assessment of progressive collapse resistance of a chord dome roof with suspended substructure in the main hall of Zhangjiaiie Circus City [J].Building Structure, 2022, 52(16): 37-44.

[6] Yu Jinghai, Wang Zhengkai, Yan Xiangyu, et al. Structural design of suspend-dome structure roof of new gymnasium of Tianjin University of Traditional Chinese Medicine [J]. Building Structure, 2015, 45(16): 1-5+90.

[7] Qu Tong, Chen Jinyu, Tan Jian. Progressive collapse resistance analysis on conjoined suspend-dome structure of Zhaoqing New District Stadium [J]. Building Structure, 2016, 46(21)：75-79.

[8] Liu Renjie, Zou Yao, Xue Suduo, et al. Influence on static performance of loop-free suspend-dome after removal of cables [J]. Journal of Building Structures, 2020, 41(S1): 1-9.
[9] Yuan Xingfei, Dong Shilin. New forms and initial prestress calculation of cable domes [J]. Engineering Mechanics, 2005, (02)：22-26.
[10] Dong Shilin, Wang Zhenhua, Yuan Xingfei. Static behavior analysis of a space structure combined of cable dome and single-layer lattice shell [J]. Journal of Building Structures, 2010, 31(03): 1-8.
[11] Zhang Ailin,Bai Yu,Liu Xuechun,et al. Static behavior analysis of new-type ridge tube cable dome with annular struts[J]. Spatial Structures,2017,23(03)：11-20.
[12] Sun Guojun, Li Xiaohui, Xue Suduo, et al. Experiment on Self-Vibration Characteristics of Levy-Type Rigid Bracing Dome [J]. Journal of Tianjin University (Science and Technology), 2019, 52(07): 719-724.
[13] Lv Hui, Chu Yiyi, Dong Shilin, et al. Static performance and parameter analysis of large-opening drum- honeycomb-type cable dome with quad-strut layout [J].Spatial Structures, 2023, 29 (03).
[14] Hui Lv, Hao Zhang, Zhong-Yi Zhu, Shi-Lin Dong and Xin Xie. Structural morphology and dynamic characteristics analysis of drum-shaped honeycomb-type iii cable dome with quad-strut layout [J]. Advanced Steel Construction, 2024, 1 (20): 81-92.
[15] LV H, CHEN Z Q, DONG S L, et al. Analytical Study of Structural Conformation and Prestressing State of Drum-Shaped Honeycomb Quad-Strut Cable Dome Structure with Different Calculation Methods[J]. Buildings, 2024, 14(1): 179.
[16] LV H, LIU D W, DONG S L, et al. Conformation and Static Performance Analysis of Pentagonal Three-Four Strut Hybrid Open-Type Cable Dome[J]. Advanced Steel Construction, 2023, 19(4): 403-410.
[17] Ministry of Housing and Urban-Rural Development of the People's Republic of China. Code for Seismic Design of Buildings：GB50011-2010 [S].China Architecture & Building Press, 2010.
[18] Ministry of Housing and Urban-Rural Development of the People's Republic of China. Technical specification for space frame structures：JGJ 7-2010 [S]. China Architecture & Building Press, 2010.
[19] Ministry of Housing and Urban-Rural Development of the People's Republic of China. Standard for Design of Steel Structures：GB50017-2017 [S]. China Planning Press, 2017.